Quantum-Chemical Modeling and Analysis of the Vibrational Structure in the Phosphorescence Spectrum of C_{60}

Maria Grazia Giuffreda, Fabrizia Negri,* and Giorgio Orlandi*

Department of Chemistry "G. Ciamician", University of Bologna, Italy

Received: June 6, 2001; In Final Form: July 19, 2001

The phosphorescence spectrum of C_{60}, recently obtained in alkane and in Xe matrixes at low temperature, has been modeled by means of semiempirical quantum chemical calculations. The $T_1 \rightarrow S_0$ transition in the unperturbed molecule is symmetry as well as spin multiplicity forbidden. The intensities of the false origins due to inducing modes have been calculated in terms of the Herzberg−Teller mechanism combined with an expansion over spin−orbit perturbations. To date, this is the first modeling of the phosphorescence spectrum of C_{60} entirely based on computed molecular parameters. Thus, the analysis of the spectrum is based not only on vibrational frequencies, but also on the comparison between computed and observed vibronic intensities. The calculations indicate that the vibrational structure is dominated by false origins due to modes of h_u, g_u, and t_{1u} symmetry, but contains also a number of combination bands based mainly on the Jahn−Teller active $h_g(1)$ mode.

1. Introduction

The characterization of the lowest triplet states of molecules is a fundamental step to give a satisfactory interpretation and, possibly, to improve time-dependent nonlinear optical properties. From this point of view, C_{60} is a very promising candidate as a material for optical limiting devices[1−3] because of the sufficiently long lifetime of its lowest triplet state, T_1, (about 400 μs[4,5] in hydrocarbon matrixes below 10 K), of the high efficiency ($\phi_T = 0.97$ [3,6,7]) of the $S_1 \rightarrow T_1$ intersystem-crossing (isc), and of the fairly high transient molar extinction coefficient in the visible spectral region.[2,3] In fact, C_{60} is almost transparent in the visible region under low optical intensities, when the molecules are virtually all in the ground state, but becomes more and more absorbing when it is exposed to light of increasing intensity and a larger number of molecules are brought to the T_1 state.

Similarly to the lowest singlet states,[8,12] also the lowest triplet states are of g-type and calculations indicate that the T_1 state belongs to the T_{2g} irreducible representation.[8] Therefore the phosphorescence process is symmetry and spin-multiplicity forbidden in C_{60} and it is induced by spin−orbit and vibronic interactions. As a consequence, this transition is extremely weak and can be enhanced by the external heavy-atom effect, that is, by dispersion of C_{60} in matrixes containing heavy atoms. Furthermore, if the symmetry remains I_h, the 0−0 band will be missing and, in analogy with the fluorescence spectrum, it can be anticipated that most of the vibrational structure will consist of false origins associated to HT inducing modes, along with a few combination bands based on inducing modes and Franck−Condon (FC) active totally symmetric (a_g) modes or JT active h_g modes. A more quantitative and detailed estimate of the above contributions can only be obtained from the computation of molecular parameters and couplings followed by the modeling of vibronic intensities. This is the subject of the present study.

Thus, in the framework of our work aiming at analyzing the electronic spectra of fullerenes,[8,9,11−16] in this paper we model and discuss the vibronic structure of the phosphorescence spectrum of C_{60} on the basis of quantum chemical calculations of vibronic intensities. The analysis is carried out along the same lines followed in the interpretation of the phosphorescence spectrum of C_{70} [16] and of some disklike aromatic molecules.[17]

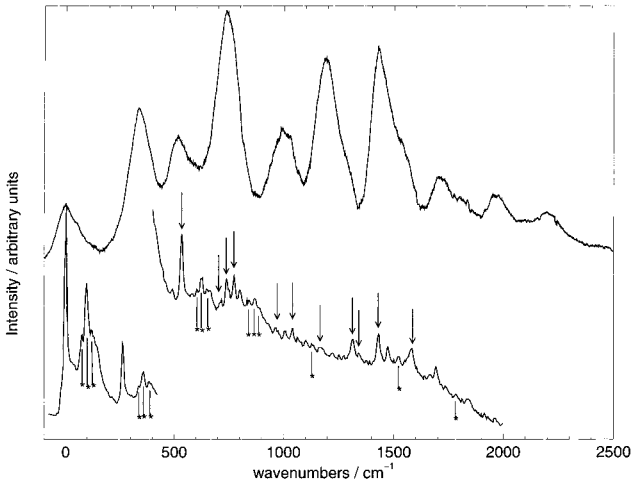

Figure 1. The phosphorescence spectrum of C_{60} in cyclohexane−decalin matrix at 1.5 K, from ref 22, top, and in Xe matrix at 30 K, from ref 20, bottom.

The phosphorescence spectra of C_{60} presently available, taken in matrixes at low temperature, are sufficiently well resolved to warrant a detailed discussion of them. Several groups have studied the phosphorescence spectra of C_{60}.[4,5,18−21] Our analysis will be based on the recent spectra of Sassara et al.[20] and of Groenen and co-workers[5,22] depicted in Figure 1. The first, shown at the bottom of Figure 1, was taken in Xe matrix at 30 K and shows a strong 0−0 band followed by FC progressions, which indicate that the heavy-atom interactions lower the effective molecular symmetry. In addition, it displays a very fine structure that reveals several HT-induced bands in the spectral interval 700−2000 cm^{-1}. The second spectrum, shown at the top of Figure 1 and taken in the cyclohexane−decalin

* Authors to whom correspondence should be addressed.

10.1021/jp0121769 CCC: $20.00
Published on Web 09/19/2001

TABLE 1: Energies (eV) and Symmetry Type of the Lowest Triplet States of C_{60} Computed by CNDO/S-CI[a]

n	sym.	*E*(eV)[b]	*E*(eV)[b]	*E*(eV)[c]	*E*(eV)[d]	expt
1	$1T_{2g}$	2.17	2.17	1.89	1.41	1.58[e],1.55[f]
2	$1G_u$	2.96	2.96	2.32	1.83	
3	$1T_{1g}$	2.53	2.53	2.35	1.95	
4	$1H_g$	2.89	2.89	2.61	2.09	
5	$1T_{1u}$	3.05	3.05	2.69	2.30	
6	$1G_g$	2.90	2.90	2.74	2.30	
7	$1T_{2u}$	3.04	3.04	2.78	2.41	
8	$1H_u$	3.34	3.34	2.88	2.47	

[a] Computed at the ground-state equilibrium geometry. [b] 196 (14*14) configurations in the CI, with Pariser electronic repulsion. [c] 1050 (35*30) configurations in the CI, with Pariser electronic repulsion.[d] 930 (31*30) configurations in the CI, with Mataga-Nishimoto electronic repulsion. [e] From ref 20. [f] From ref 5.

(CD) matrix at 1.5 K, has a lower resolution, but its 0−0 band is weak, as it should be for very weakly distorted molecules. This spectrum extends up to 2200 cm^{-1} and most of its intensity is found in the HT false origins and in combination bands based on them. Thus, the two spectra are complementary and together present a reasonable number of spectral features.

The paper is organized as follows. In Section 2 we describe how our calculations were performed. In Section 3 we report our results on the lowest triplet states, on the vibronic activities of inducing and FC active modes. In Section 4 we apply them to the analysis of the experimental spectra.

2. Methods of Calculations

Electronic energies and transition dipole moments have been obtained by using the semiempirical CNDO/S Hamiltonian[23] which has been widely employed in the study of unsaturated molecules and, particularly, to the interpretation of singlet state spectroscopy of C_{60}.[9,12] The Self-Consistent-Field (SCF) calculation of Molecular Orbitals (MOs) was followed by a Configuration Interaction (CI) calculation in which only Singly Excited (SE) configurations were taken into account. In some of the calculations of triplet states energies (see Table 1) the two-centers electron repulsion integrals were evaluated according to the Pariser formula. The CI treatment included 196 SE configurations arising from the promotion of an electron from the space of the 14 highest occupied MOs (h_u, h_g, and g_g molecular orbitals) to the space of the 14 lowest unoccupied MOs (t_{1u}, t_{1g}, t_{2u}, and h_g molecular orbitals). To check the validity of this description we performed CI calculations of larger sizes that included 1050 (35 × 30) SE configurations and did not find appreciable differences in the energy ordering of lower electronic states. We also performed CI calculations by employing 930 (31 × 30) SE electronic configurations with the Mataga-Nishimoto (MN) approximation for repulsion integrals. The resulting energy ordering of the triplet states was the same as with the previous calculations, but the energy of the T_1 state is closer to the measured value. Therefore, we choose to perform all the calculations of intensity borrowing with this CI. An extension of the CI treatment to doubly excited configurations, which must be considered with caution when a semiempirical Hamiltonian is used because of the danger of overaccounting for electronic correlation, is not necessary in this case. In fact, we are interested only in T_1 and, since this state is found to be lower than the next triplet of the same symmetry by at least 1 eV, its wave function cannot be appreciably modified by the inclusion of double excitations.

The calculations were run at the equilibrium structure of C_{60} obtained in our previous study,[8] that is, with the bond lengths $\boldsymbol{R}_{CC(66)} = 1.411$ Å and $\boldsymbol{R}_{CC(65)} = 1.471$ Å.

In analogy with the procedure followed to simulate the phosphorescence spectra of C_{70} [16] and of some disklike aromatic molecules,[17] the spin−orbit coupling integrals were evaluated in the one electron approximation, by taking into account only the one-center contributions, according to the Jaffé approach.[32]

The spin−orbit induced transition dipole moments between the ground-state S_0 and the triplet state $T_{j\alpha}$ ($\alpha = 1,0,-1$ indicates the spin component) is expressed by the perturbation expansion over the intermediate states S_k and $T_{m\alpha}$, respectively,

$$\boldsymbol{M}_{0,j\alpha} = \Sigma_k \boldsymbol{M}_{0k}\boldsymbol{V}_{k,j\alpha}/(\boldsymbol{E}_j - \boldsymbol{E}_k) + \Sigma_m \boldsymbol{M}_{jm}\boldsymbol{V}_{0,m\alpha}/(\boldsymbol{E}_0 - \boldsymbol{E}_m) \quad (1)$$

In the first term of eq 1 $\boldsymbol{M}_{0k}$ is the transition moment between the states S_0 and S_k while $\boldsymbol{V}_{k,j\alpha}$ is the spin−orbit interaction between S_k and $T_{j\alpha}$. Similarly, in the second term of eq 1 $\boldsymbol{M}_{jm}$ is the transition moment between the states $T_{j\alpha}$ and $T_{m\alpha}$ and $\boldsymbol{V}_{0,m\alpha}$ is the spin−orbit interaction between S_0 and $T_{m\alpha}$.

In the case of C_{60}, the transition moment derived from eq 1 vanishes by symmetry. To obtain the intensities of the false origins of the $S_0 \rightarrow T_1$ symmetry-forbidden transition, we calculated the numerical derivatives of the corresponding transition moments with respect to all the normal coordinates $\boldsymbol{Q}_k$ that may be active by symmetry, i.e., may have nonzero derivative. From these induced electronic transition moments, M^k_{01}, the vibronic transition moments of the false origins corresponding to the ν_k fundamentals $\boldsymbol{M}^k_{00,11}$ can be readily obtained (see also refs 16 and 17).

The normal coordinates $\boldsymbol{Q}_k$ required to calculate the induced electronic moments M^k_{0j} were computed by the QCFF/PI Hamiltonian[25] which was shown to be able to describe the vibrational force field of unsaturated hydrocarbons[26] and fullerenes[8,11,27] very satisfactorily.

The oscillator strength $\boldsymbol{f}$ for each false origin is obtained from the usual relationship[28a]

$$\boldsymbol{f} = (1/3)\boldsymbol{A}\nu\mathbf{M}^2 \quad (2)$$

where $\boldsymbol{A} = 4.7 \times 10^{29}$, ν is the wavenumber for the corresponding vibronic transition, and $\mathbf{M}$ (that is, $M^k_{00,11}$) is the corresponding transition dipole moment in esu.

In general, also the FC mechanism, which is based on squared overlap of vibrational wave functions of the initial and final electronic states, can contribute to the vibrational structure of electronic transitions. This contribution comes mainly from TS and JT active vibrations and it is due to the displacement of the excited-state equilibrium geometry with respect to the ground state. Since in the T_{2g} state the JT distortions occur along h_g normal coordinates, the FC active modes in the C_{60} phosphorescence include h_g modes beside a_g modes.

The γ parameters required to estimate the FC activities in the phosphorescence were taken from our previous studies,[8,15] that employed two different sets of MOs and CI of different sizes to describe the T_1 state.

In the harmonic approximation, the intensity of the vth member of the progression of the ith FC active mode is given by the relation

$$\boldsymbol{I}_i(v) = \exp(-\gamma_i)\,(\gamma_i)^v/v! \quad (3)$$

According to eq 3 the ratio between the intensity of a member of the progression in the ith FC active mode and the 0−0 band is given by

$$I_i(v)/\boldsymbol{I}(0\text{-}0) = (\gamma_i)^v/v! \quad (4)$$

Similarly, eq 4 holds also for the ratio between the intensity of the members of a progression built on a false origin and the intensity of the false origin.

Summing together the oscillator strengths of all the false origins one gets the oscillator strength of the $T_1 \rightarrow S_0$ transition, f_T. From this parameter the radiative rate constant, k_{Ph}, of the phosphorescence can be obtained:[28b]

$$k_{Ph} = 0.656\nu^2 n^3 f_T \qquad (5)$$

where n is the solvent refraction index, ν is the wavenumber associated with the $T_1 \rightarrow S_0$ energy gap, and f_T is the total oscillator strength. This rate constant can be compared with the corresponding experimental value.

3. Results

a. Electronic States. In Table 1 we list energy and symmetry labels of the lowest triplet levels computed with three different CI calculations based on the CNDO/S Hamiltonian. All the three CNDO/S calculations assign the lowest triplet state, T_1, to the T_{2g} symmetry representation. This state is computed to be 2.17 eV, 1.89 eV, and 1.41 above the ground state for the three CI, respectively. Both the energy gaps obtained by the Pariser repulsion are larger than the values observed in inert matrixes, of 1.55 eV [5] and 1.58 eV,[20] but the agreement is better when the MN repulsion is used.

According to our calculations the T_1 state is at least 0.4 eV below the next two triplets, which belong to G_u and T_{1g} symmetry. At variance with the lowest singlet states of C_{60} which are computed to be quasi-degenerate,[9,12] the energy gap between T_1 and T_2 is sufficiently large to ensure that the calculated ordering is reliable, that is, that T_1, the state responsible for the phosphorescence, belongs to the T_{2g} symmetry type. As it will be seen shortly, the computed vibronic structure of the phosphorescence spectrum supports this assignment.

b. Intensity of HT Vibronically Induced and FC Bands in Phosphorescence. As noted above, since in I_h symmetry the triplet spin wave functions transform as T_{1g}, and the dipole moment Cartesian components transform as T_{1u}, the T_1- - -S_0 transition moment is symmetry as well as spin-multiplicity forbidden. Thus, this transition is induced by spin−orbit coupling combined with vibronic perturbations mediated by modes belonging to the g_u, t_{2u}, t_{1u} and h_u symmetry types. Each of the modes belonging to these species may give rise to a false origin and may thus contribute to the vibrational structure of the phosphorescence spectrum of C_{60}. There are 6 g_u, 5 t_{2u}, 4 t_{1u} and 7 h_u vibrations which need to be considered as possible promoters of false origins. The list of calculated and experimental frequencies and of the induced phosphorescence oscillator strength for each false origin is given in Table 2. The oscillator strengths presented include the contributions of all the members of degenerate vibrations.

The largest vibronic activity is found associated with the h_u modes with experimental frequencies of 403, 525, 738, and 1566 cm^{-1}, the g_u modes of 776, 963, 1315 cm^{-1} frequency and the t_{1u} mode of 525 cm^{-1} frequency. The total oscillator strength of the C_{60} phosphorescence, which is simply the sum of the oscillator strength of each false origin, amounts to 17.2×10^{-10}. Thus, the oscillator strength of C_{60} is of similar size of that calculated for C_{70} (16.4×10^{-10}).

In fullerenes, the FC mechanism was found to be rather inefficient, in other words, very few modes yield progressions or contribute to combination bands. This is evident in the fluorescence and absorption spectra of C_{60} in which little vestiges were found only for one TS mode and one h_g mode[1,2,4,8,12] and, more pertinent to present discussion, in the EEL spectrum of the lowest triplet state.[15] A plausible explanation is that the electronic excitation, being spread on a large system, produces relatively small distortion of the equilibrium geometry. Furthermore, this distortion is distributed over a large number of internal coordinates. Note also that the distortion of the minimum of the potential energy surface along the h_g modes is responsible for the symmetry lowering to the point group D_{5d}.[15,29]

The γ values which we obtained in refs 20,27, based on MOs optimized for S_0 and T_1, respectively, and on different CI sizes, are reported in Table 3 along with computed and observed vibrational frequencies. The computation of the molecular distortion along TS and JT active modes for an excited state of a molecule of the size of fullerenes is obviously a formidable problem. Thus, it is not surprising that the computed γ values

TABLE 2: Computed Oscillator Strengths (f) of the False Origins of the $T_1(T_{2g}) \rightarrow S_0(A_g)$ Transition of C_{60}[a]

sym	n	ν expt[b]	ν calcd[c]	ν calcd[d]	$f^* 10^{10}$
t_{1u}	1	525	527	504	0.33
	2	578	586	605	0.07
	3	1180	1218	1186	0.05
	4	1430	1462	1429	0.22
t_{2u}	1	354	337	322	0.10
	2	715	716	632	0.19
	3	1037	993	985	0.07
	4	1190	1228	1235	0.20
	5	1540	1535	1496	0.07
g_u	1	345	349	333	0.19
	2	757	748	748	0.08
	3	776	782	755	0.31
	4	963	975	992	0.34
	5	1315	1334	1348	0.46
	6	1410	1452	1478	0.23
h_u	1	403	399	379	0.32
	2	525	530	491	0.63
	3	667	662	745	0.10
	4	738	741	666	0.49
	5	1215	1231	1224	0.06
	6	1342	1363	1380	0.09
	7	1566	1569	1563	1.14

[a] Calculated at the ground-state equilibrium geometry, with the CI of 930 configurations and the MN electronic repulsion. [b] Taken from ref 30 with a few reassignments as proposed in refs 11 and 12. [c] DFT frequencies from ref 33. [d] Frequencies calculated by a modified QCFF/PI Hamiltonian, from ref 11.

TABLE 3: Franck-Condon Parameters γ for the $T_1(T_{2g}) \rightarrow S_0(A_g)$ Transition for the a_g and h_g Modes Computed by the QCFF/PI Hamiltonian

sym	n	ν expt[a]	ν calcd[b]	ν calcd[c]	γ^d	γ^e
a_g	1	494	495	513	0.00	0.00
	2	1468	1504	1442	0.22	0.11
h_g	1	266	259	240	1.43	0.20
	2	431	425	405	0.00	0.00
	3	709	711	633	0.00	0.00
	4	772	783	794	0.17	0.02
	5	1095	1120	1124	0.00	0.00
	6	1248	1281	1243	0.00	0.00
	7	1421	1450	1435	0.22	0.01
	8	1574	1578	1562	0.34	0.03

[a] Taken from ref 30 with a few reassignments as proposed in refs 11 and 12. [b] DFT frequencies from ref 33. [c] Frequencies calculated by a modified QCFF/PI Hamiltonian, from ref 11. [d] Computed by a CI based on MOs optimized for the triplet state, from ref 15. [e] From the displacement parameters B of ref 8.

are dependent on the level of the calculations. Nevertheless, both calculations indicate that only the $h_g(1)$ mode at 266 cm^{-1} should stand out prominently in the spectrum, and that also the $a_g(2)$ and the $h_g(8)$ modes at 1468 and 1574 cm^{-1} may contribute through combination bands to the vibrational structure.

4. Assignment of the Observed Phosphorescence Spectra

As noted above, the phosphorescence spectrum of C_{60} in the gas phase is both symmetry and spin-multiplicity forbidden. It is thus extremely weak.

Most of the phosphorescence spectra available were recorded in low-temperature matrixes containing heavy atoms to enhance spin−orbit interaction and thus radiative and nonradiative singlet−triplet transitions. Fortunately, the heavy-atom effect enhances the phosphorescence more strongly than the $T_1 \rightarrow S_0$ isc, and thus increases the efficiency of the phosphorescence process. The spectra of Zeng et al.,[19] taken in a matrix containing MCH/MTHF ethyliodide, and of Hung et al.,[21] measured in Ne matrix doped with Xe, belong to this group. Recently, Sassara et al.[20] reported for C_{60} an intense and highly resolved phosphorescence spectrum taken in a Xe matrix. One important side effect of these matrixes is to lower effectively the symmetry of C_{60}, with the consequence that the phosphorescence spectrum becomes symmetry allowed. The spectrum in Xe matrix (see Figure 1, bottom) shows a strong 0−0 band, at 12.714 cm^{-1}, followed by a progression of the $h_g(1)$ mode on top of which one can recognize the weak bands due to u-type inducing modes. Therefore, it does not provide information on the vibrational structure of the isolated molecule in the 0−700 cm^{-1} spectral range. In the 700−2000 cm^{-1} frequency region several bands are identified that can be due to the HT inducing modes, combination bands, and to fundamentals of FC active modes. As discussed by the authors,[20] the observed spectrum is the superposition of the spectra of two sites, the second of which has a broader emission shifted about 100 cm^{-1} to the red, that can be easily separated. In Figure 1 we have indicated with an asterisk the bands due to the second site.

The phosphorescence spectrum measured at 1.5 K in a CD matrix by van den Heuvel et al.,[5] and extended recently over a larger spectral range,[22] is weak and less resolved than the spectrum in the Xe matrix, presumably because it results from emitting molecules experiencing many different environments. However, it has a great advantage: its 0−0 band is weak and thus all the observed vibronic bands should be assigned to HT active modes or to combination bands based on them. This spectrum, which starts from the 0−0 band at 12530 cm^{-1}, is shown at the top of Figure 1.

All the bands observed in the two spectra are collected in Table 4 and are now discussed on the basis of our intensity calculations and of the experimental vibrational frequencies of Schettino et al.[30]

In the following discussion we shall take as reference the spectrum measured in CD matrix, since it is more compatible with the I_h symmetry and thus is more directly comparable with our calculated spectrum, which is pertinent to an isolated molecule. However, we shall emphasize the common features of the two experimental spectra and we shall resort to the more resolved Xe matrix spectrum to discuss in more detail the assignment proposed on the basis of our calculations.

A picture of the phosphorescence spectrum simulated on the basis of calculated vibronic intensities of the HT and FC active modes is shown in Figure 2. The simulation is performed by using two Lorentzian bandwidths of 50 and 5 cm^{-1} which allow to mimic the broadening observed in the experimental spectra

TABLE 4: Vibrational Bands of C_{60} Phosphorescence Spectra and Their Assignments

CH/D 1.5 K[a]		Xe 30 K[b]		
ν(cm^{-1})	$\Delta\nu$	ν(cm^{-1})	$\Delta\nu$	assignment[c]
12530	0	12714	0	0−0
	345			345 $g_u(1)$, 354 $t_{2u}(1)$, 403 $h_u(1)$
	520			525 $h_u(2)$, 525 $t_{1u}(1)$, 2*266 $h_g(1)$
			710	715 $t_{2u}(2)$
	745		737	738 $h_u(4)$
			771	776 $g_u(3)$; 772 $h_g(4)$,
			959	963 $g_u(4)$
	995		1007	738+ 266 $h_g(1)$
	1030		1037	776+ 266 $h_g(1)$, 1037 $t_{2u}(3)$
	1190		1172	1180 $t_{1u}(3)$, 1190 $t_{2u}(4)$
			1312	1315 $g_u(5)$
			1338	1342 $h_u(6)$
	1435		1425	1430 $t_{1u}(4)$, 1410 $g_u(6)$; 1421 $h_g(7)$
			1468	1468 $a_g(2)$
	1531		1573	1566 $h_u(7)$, 1315+ 266 $h_g(1)$; 1574 $h_g(8)$
	1710		1686	1430+ 266 $h_g(1)$, 1410+ 2*266 $h_g(1)$
			1734	1468+ 266 $h_g(1)$
	1840		1839	1566+ 266 $h_g(1)$, 1315+ 2*266 $h_g(1)$; 1574+ 266 $h_g(1)$
	1935		1960	1430+ 2*266 $h_g(1)$, 1410+ 2*266 $h_g(1)$
	2185			745+1468 $a_g(2)$

[a] From refs 5 and 22. [b] From ref 20; note that the band at 845 cm^{-1}, without counterpart in the list of inducing modes (see Table 2), has been attributed to the 738 cm^{-1} $h_u(4)$ band of site 2. [c] Based on the calculations presented in this work; experimental vibrational frequencies are taken from ref 30.

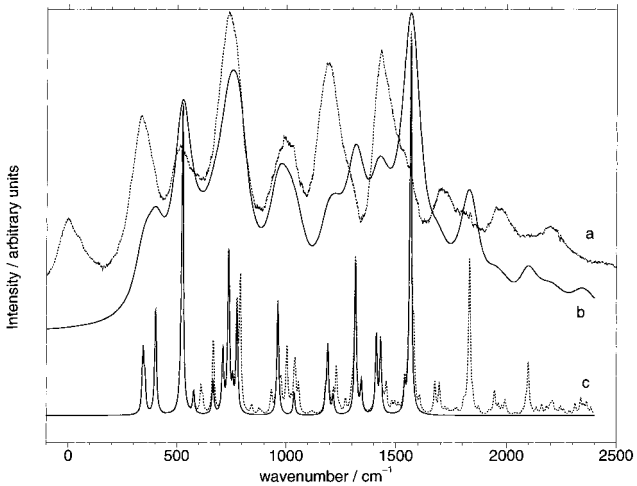

Figure 2. Comparison between simulated and observed experimental spectra of C_{60}. (a) the experimental spectrum obtained in the CD matrix at 1.5 K;[22] (b) the phosphorescence spectrum simulated with a bandwidth of 50 cm^{-1}; (c) the phosphorescence spectrum simulated with a bandwidth of 5 cm^{-1}. The solid line bands are HT-induced false origins discussed in the text. The remaining bands are progressions and combinations of FC bands built on false origins.

in CD matrix[22] (spectrum a, in Figure 2) and in Xe matrix,[20] respectively.

The solid line bands, in the high-resolution spectrum (spectrum c, in Figure 2), correspond to HT-induced false origins. The dotted line bands are progressions of TS and JT modes built on the false origins. To compare our computed spectrum with the experimental spectrum obtained in the Xe matrixes,[20] we artificially included in the simulated spectrum of Figure 3 a strong 0−0 band and the associated progressions of TS and JT active modes (see the bottom of Figure 3). In the same way as in the experimental spectrum[20] shown in Figure 3, the intensity of the 0−450 cm^{-1} frequency range of the simulated spectrum is reduced by a factor of 1/3.

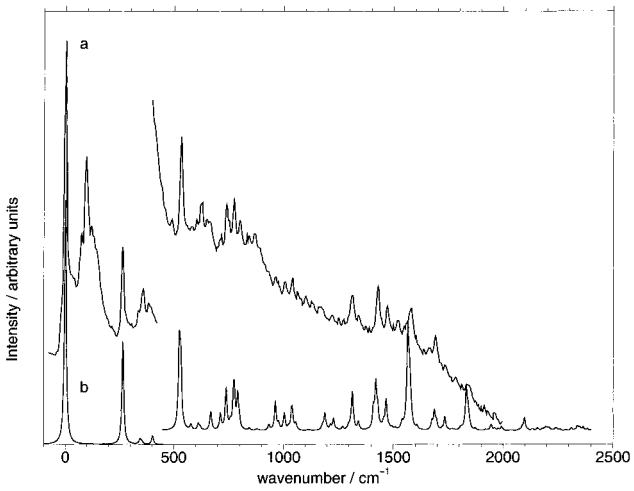

Figure 3. Comparison between simulated and observed experimental spectra of C_{60}. (a) the experimental spectrum obtained in the Xe matrix at 30 K;[20] (b) the phosphorescence spectrum simulated with a bandwidth of 5 cm^{-1}. A strong 0−0 band was added to the computed intensities as discussed in the text.

The computed values of the γ parameters of TS and JT modes were used as a guide in the simulations of the phosphorescence spectra of Figures 2 and 3. The actual values employed were adjusted in order to improve the fitting of the experimental spectrum and resulted to be intermediate between the two computed sets[8,15] in Table 3.

Conversely, the HT-induced intensities presented in Figures 2 and 3 correspond exactly to the computed values. Finally, to make the comparison with the experimental spectrum easier, the experimental vibrational frequencies from ref 30 were used to build the simulated spectra.

The first vibronic band following the 0−0 band in the spectrum in CD matrix is centered at 345 cm^{-1} and is roughly 150 cm^{-1} wide at half-height. From the comparison with the calculated oscillator strengths, it appears to obtain its intensity from three fundamentals of 345, 354, and 403 cm^{-1} corresponding to the $g_u(1)$, $t_{2u}(1)$, and $h_u(1)$ modes, respectively. Unfortunately, the spectrum obtained in Xe matrixes does not give additional information since the bands observed in this region are due to the second site (see Figure 1).

The second vibronic band in the CD spectrum, observed at 525 cm^{-1}, is naturally assigned to the two modes $t_{1u}(1)$ and $h_u(2)$, both with frequency of 525 cm^{-1}. While the frequencies of active inducing modes correspond rather well to the frequencies of the vibronic bands observed in the phosphorescence spectrum, their relative intensities are not always predicted accurately. This is the case of the intensity of the 525 cm^{-1} band which is comparatively overestimated by the calculations. Again, the spectrum in the Xe matrix does not provide information on HT vibronically induced bands since the strong band observed at 532 cm^{-1} is due to the overtone of the $h_g(1)$ JT active mode and completely overrides any possible weak band in the same frequency region.

The third vibronic band observed in the CD matrix is centered at 745 cm^{-1} and is the most intense. It includes the three bands observed at 710, 737, and 771 cm^{-1} in the Xe matrix.[20] These three bands, as well as the remaining bands assigned completely or partially to HT inducing modes, are indicated with an arrow in Figure 1. Our calculations show that these bands derive their intensity from the $t_{2u}(2)$, $h_u(4)$, $g_u(3)$ inducing modes whose experimental frequencies are 715, 738, and 776 cm^{-1},[30] respectively.

The next band, showing features at 995 and 1030 cm^{-1}, carries roughly half of the intensity of the previous band and includes the three bands observed in the Xe matrix spectrum at 959, 1007, and 1037 cm^{-1}. The first is assigned to the $g_u(4)$ fundamental, of 963 cm^{-1}, while the other two bands are ascribed to the combination bands of the 266 cm^{-1} $h_g(1)$ mode with the $h_u(4)$ and $g_u(3)$ inducing modes. However, according to our results, a weak contribution to the 1037 cm^{-1} band may come also from the $t_{2u}(3)$ mode whose experimental frequency is exactly 1037 cm^{-1}.

The broad band with the maximum at 1190 cm^{-1}, extending from 1100 to 1300 cm^{-1}, is one of the prominent bands of the CD spectrum. It comprises the weak bands at 1172 and 1338 cm^{-1} and the relatively intense band at 1312 cm^{-1} observed in the Xe matrix spectrum.[20] The correspondence between the two spectra in this interval is modest since much more intensity is observed in the CD spectrum compared to the Xe matrix spectrum, as it can be seen in Figure 1. Our calculations, together with the assignment of vibrational frequencies, are in a better agreement with the spectrum taken in Xe matrix. Indeed, as shown in Table 4 and Figure 2, the most intense band is predicted at 1312 cm^{-1} and is assigned to the $g_u(5)$ mode. Some activity is predicted also for the $t_{1u}(3)$ and $t_{2u}(4)$ modes at 1180 and 1190 cm^{-1}, respectively. However, the intensity calculated at 1190 cm^{-1} is much weaker than the intensity observed in the CD spectrum. Conversely, our calculations account very well for the bands observed in the Xe matrix spectrum.

The band with the peak at 1435 cm^{-1} and a shoulder at 1531 cm^{-1}, comprises the bands observed at 1425 and 1573 cm^{-1} in the Xe matrix spectrum.[20] According to our calculations, the first can be assigned to the $g_u(6)$ (1410 cm^{-1}) and $t_{1u}(4)$ (1430 cm^{-1}) modes, while the second is attributed to the $h_u(7)$ fundamental (1566 cm^{-1}) and to the combination band 266 +1310 cm^{-1}. In both spectra the intensity of the $h_u(7)$ fundamental is not especially prominent: clearly, our calculations that assign to this mode the largest HT activity, overvalue considerably its intensity. Since the intensity of the inducing mode at 1566 cm^{-1} was overestimated also in the simulation of the C_{70} phosphorescence spectrum,[16] it may be inferred that the CNDO/S Hamiltonian tends to exaggerate systematically the vibronic activity of C═C stretching modes in phosphorescence. There are several reasons to explain this overestimate, among these the parametrization chosen which describes more correctly the $\pi\pi^*$ states, the size of the configuration space adopted, and the approximation in the derivation of spin−orbit coupling.

The band at 1710 cm^{-1}, with a shoulder at 1840 cm^{-1}, and the band at 1935 cm^{-1} in the CD matrix spectrum, can only be combinations bands. Not surprisingly, as shown in Table 4, they involve the $h_g(1)$ mode. For the last band in the spectrum in CD matrix, observed at 2185 cm^{-1}, many attributions are possible; one of them is the combination of the $h_u(4)$ with the TS $a_g(2)$ mode. The FC activity of the $a_g(2)$ mode is indeed supported by our calculations since this is predicted to be one of the most active modes beside the $h_g(1)$ vibration (see Table 3).

In summary, the assignment presented in this work, on the basis of computed phosphorescence intensities, suggests a few changes with respect to the analysis proposed by Sassara et al.,[20] as it can be seen from the comparison of our Table 4 with the part of Table 1 dealing with the emission of the dominant site 1 in ref 20. The main changes are the following:

(i) the band at 771 cm^{-1} is assigned by us as due, at least partially, to the $g_u(3)$ false origin;

(ii) the 841 cm^{-1} band is attributed to site 2, where it corresponds to a band of 737 cm^{-1};

(iii) the 1037 cm^{-1} band is reassigned in keeping with our attribution of the 771 cm^{-1} band; furthermore, as already mentioned above, the weak $t_{2u}(3)$ false origin can be expected at exactly the same frequency;

(iv) the 1468 cm^{-1} band can be due only to the $a_g(2)$ fundamental; the alternative assignment to the $h_g(7)$ fundamental[20] is much less plausible because the frequency of this mode,[30] 1421 cm^{-1}, does not correspond well to the frequency of the observed band.

Although in the above discussion we have considered only false origins and combination bands depending on them, in Table 4 and in Figure 3 we have reported also bands observed in the Xe matrix spectrum that are due to the FC mechanism and based on the true origin. Beside the ubiquitous $h_g(1)$, the $a_g(2)$ mode of 1468 cm^{-1} appears undoubtedly in the spectrum as the sole responsible of the band observed at 1468 cm^{-1}. Also the $h_g(4)$, $h_g(7)$, and $h_g(8)$ modes may contribute to the intensity of the bands observed at 771, 1425, and 1573 cm^{-1}, respectively. A contribution to the latter band from the JT active mode $h_g(8)$, as proposed in ref 20, is supported by our results and might explain in part the stronger intensity in this frequency region in the Xe matrix spectrum, compared with the CD matrix spectrum.

To check the accuracy of our calculated induced intensities, we computed the average radiative rate constant for each of the three equivalent triplet sublevels by using eq 5. The cumulative oscillator strength, f_T, of the false origins amounts to $f_T = 5.7 \times 10^{-10}$. The value of the refraction index of MCH is 1.4 at 20 °C,[31] and becomes 1.53 at 1.5 K by using the average temperature correction factor.[32] By estimating the average wavenumber ν of the phosphorescence vibronic structure to be the 12000 cm^{-1}, we get a rate constant k_{Ph} of 0.19 s^{-1} for the phosphorescence process, very similar to the value of 0.11 s^{-1} calculated for C_{70}.[16] The computed rate constant, combined with the experimental lifetime of 0.4 ms,[5] leads to an estimated phosphorescence quantum yield of 0.76×10^{-4}. Although, to our knowledge, a measure of this parameter is not available, the calculated value appears to be qualitatively correct. In fact, it is about 2 orders of magnitude smaller than the calculated quantum yield of C_{70} (5.83×10^{-3}),[16] and this agrees with the particular weakness of the C_{60} phosphorescence and with the consequent difficulty of observing it.

5. Conclusions

We have modeled the vibronic structure of the phosphorescence spectrum of C_{60} on the basis of quantum-chemically computed molecular parameters and couplings. The calculations indicate that the vibrational structure of the phosphorescence spectra of unperturbed C_{60} is dominated by false origins which derive their intensity through spin−orbit perturbations *and* by electron−phonon coupling mediated by modes of h_u, g_u, and t_{1u} symmetry types. A number of observed bands can be attributed to combinations bands of inducing modes and FC active modes. Among the latter an important role is played by the $h_g(1)$ mode, but also the mode $a_g(2)$ contributes to the vibrational structure. The spectrum taken in Xe matrix shows an intense true origin, indicating an effective deviation of C_{60} from the I_h symmetry, beside the expected external heavy atom effect. In this spectrum, the role of FC active modes is obviously more pronounced since progressions of TS and JT active modes, built on the 0−0 band, appear with strong intensity in the spectrum.

This analysis is able to model successfully the vibrational structure of the phosphorescence spectrum of C_{60} based on the assignment of T_1 as the lowest state of T_{2g} character, as predicted by quantum chemical calculations. At the same time, it strengthens by its success the identification of the nature of the lowest excited triplet state.

The accuracy in the modeling of phosphorescence spectra of C_{60}, C_{70},[16] and some disklike molecules[17] is surprising if one considers that band intensities result from the combination of two perturbations and from a perturbative expansion where a substantial cancellation among the various terms may occur. On the other hand, it indicates once again the ability of the classical semiempirical quantum-chemical methods employed here, to evaluate correctly spectroscopic features of large aromatic and unsaturated hydrocarbons as well as of fullerenes.

Acknowledgment. Grant INTAS 97-11894 is gratefully acknowledged by F.N.

References and Notes

(1) Signorini, R.; Meneghetti, M.; Bozio, R.; Maggini, M.; Scorrano, G.; Prato, M.; Brusatin, G.; Innocenzi, P.; Guglielmi, M. *Carbon* **2000**, *38*, 1653; Maggini, M.; De Faveri, C.; Scorrano, G.; Prato, M.; Brusatin, G.; Guglielmi, M.; Signorini, R.; Meneghetti, M.; Bozio, R. *Chem. Eur. J.* **1999**, *5*, 2501.

(2) Ebbesen, T. W.; Tanigaki, K.; Kuroshima, S. *Chem. Phys. Lett.* **1991**, *181*, 501; Kaiji, Y.; Nakagawa, T.; Suzuki, S.; Achiba, Y.; Obi, K.; Shibuya, K. *Chem. Phys. Lett.* **1991**, *181*, 100.

(3) Bensasson, R. V.; Hill, T.; Lambert, C.; Land, E. J.; Leach, S.; Truscott, T. G. *Chem. Phys. Lett.* **1993**, *201*, 326.

(4) Wasielewski, M. R.; O'Neil, M. P.; Lykke, K. R.; Pellin, M. J.; Gruen, D. M. *J. Am. Chem. Soc.* **1991**, *113*, 2774.

(5) van den Heuvel, D. J.; Chan, I. Y.; Groenen, E. J. J.; Schmidt, J.; Meijer, G. *Chem. Phys. Lett.* **1994**, *231*, 111.

(6) Arbogast, J. W.; Darmanyan, A. P.; Foote, C. S.; Rubin, Y.; Diederich, F.; Alvarez, M. M.; Anz, S. J.; Whetten, R. L. *J. Phys. Chem.* **1991**, *95* (5), 11.

(7) Biczok, L.; Linschitz, H.; Walter, R. I. *Chem. Phys. Lett.* **1992**, *195*, 339.

(8) Negri, F.; Orlandi, G.; Zerbetto, F. *Chem. Phys. Lett.* **1988**, *195*, 339.

(9) Negri, F.; Orlandi, G.; Zerbetto, F. *J. Chem. Phys.* **1992**, *195*, 339.

(10) Lazlo, I.; Udvardi, L. *Chem. Phys. Lett.* **1987**, *136*, 418; Braga, M.; Larsson, S.; Rosén, A. *Astron. Astrophys.* **1991**, *245*, 232.

(11) Negri, F.; Orlandi, G. *J. Phys. B: At. Mol. Opt. Phys.* **1996**, *29*, 5049.

(12) Negri, F.; Orlandi, G.; Zerbetto, F. *J. Phys. Chem.* **1996**, *100*, 10849; Sassara, A.; Zerza, G.; Chergui, M.; Negri, F.; Orlandi, G. *J. Chem. Phys.* **1997**, *107*, 8731.

(13) Negri, F.; Orlandi, G. *J. Chem. Phys.* **1998**, *108*, 9675.

(14) Negri, F.; Orlandi, G. *Z. Phys. Chem.* **1997**, *200*, 85.

(15) Cepek, C.; Goldoni, A.; Modesti, S.; Negri, F.; Orlandi, G.; Zerbetto, F. *Chem. Phys. Lett.* **1996**, *250*, 537.

(16) Negri, F.; Orlandi, G. *J. Phys. B: At. Mol. Opt. Phys.* **1996**, *29*, 5077.

(17) Baunsgaard, D.; Harrit, N.; El Balsami, M.; Negri, F.; Orlandi, G.; Frederiksen, J.; Wilbrandt, R. *J. Phys. Chem. A* **1998**, *102*, 10007.

(18) Wang, Y. *J. Phys. Chem.* **1992**, *96*, 764; Palewska, K.; Sworakowski, J.; Chojnacki, H.; Meister, E. C.; Wild, U. P. *J. Phys. Chem.* **1993**, *97*, 12167.

(19) Zeng, Y.; Biczok, L.; Linschitz, H. *J. Phys. Chem.* **1992**, *96*, 5237.

(20) Sassara, A.; Zerza, G.; Chergui, M. *Chem. Phys. Lett.* **1996**, 26*1*, 213.

(21) Hung, W.-C.; Ho, C.-D.; Liu, C.-P.; Lee, Y.-P. *J. Phys. Chem.* **1996**, *100*, 3927.

(22) Dauw, X. L. R. Ph.D. Thesis, Leiden University, 2000.

(23) Del Bene, J.; Jaffè, H. H. *J. Chem. Phys.* **1968**, *48*, 1807.

(24) Masmanidis, C. A.; Jaffé, H. H.; Ellis, R. L. *J. Phys. Chem.* **1975**, *79*, 19; McGlynn, S. P.; Azumi, T.; Kinoshita, M. *The Triplet State*; Prentice Hall: Englewood Cliffs, NJ, 1969.

(25) Warshel, A.; Karplus, M. *J. Am. Chem. Soc.* **1972**, *19*, 5612.

(26) Warshel, A. In *Modern Theoretical Chemistry*; Schafer, H. F., II, Ed.; Plenum: New York, 1977; Vol. 7, p 153; Lasaga, A.; Aerni, R. J.; Karplus, M. *J. Chem. Phys.* **1980**, *73*, 5230; Orlandi, G.; Zerbetto, F.; Zgierski, M. Z. *Chem. Rev.* **1991**, *91*, 867.

(27) Negri, F.; Orlandi, G.; Zerbetto, F. *J. Am. Chem. Soc.* **1991**, *113*, 6037.

(28) (a) Birks, J. B. *Photophysics of Aromatic Molecules*; J. Wiley: New York, 1970; Chapter 3.7; (b) ibid., Chapters 3.7 and 4.3.

(29) Surjan, P. R.; Udvardi, L.; Nemeth, K. *J. Mol. Struct. (THEOCHEM)* **1994**, *311*, 55; Dauw X. R. L.; van der Berg, G. J. B.; van den Heuvel, D. J.; Poluektov, O. G.; Groenen, E. J. J. *J. Chem. Phys.* **2000**, *112*, 7102.

(30) Schettino, V.; Salvi, P. R.; Bini, R.; Cardini, G. *J. Chem. Phys.* **1994**, *101*, 11079.

(31) *CRC Handbook of Chemistry and Physics*; CRC Press, Inc: Boca Raton, FL, 1972.

(32) Fessenden, R. J.; Fessenden, J. S. *Organic Laboratory Techniques*, 2nd ed.; Brooks/Cole Publishing Co.: Pacific Grove, CA, **1993**.

(33) Giannozzi, P.; Baroni, S. *J. Chem. Phys*. **1993**, *100*, 8537.